Phytosome loaded with biosynthesized Ag NPs for combating bone cancer through second-order targeting of FGFR3P1 and CDK12 via insilico approach

Mathusree.I, Anandhavardini.R.K , Tharani.S ,

Pradeepa S.Y & Bindhu. J*

[1]*Department of Biotechnology, Sri Shakthi Institute of Engineering & Technology, Coimbatore,641*

Corresponding authors' details;

Dr. J. Bindhu

Associate Professor & Head
Department of Biotechnology
Sri Shakthi Institute of Engineering & Technology, Coimbatore
Email: bindhuravi.edu@gmail.com, bindhubt@siet.ac.in

Abstract

Introduction: Biosynthesized Ag NPs from the combined herbal extracts of *M. koeinji, C. longa*, and *A. sativum* are analyzed in the in-vitro treatment of bone cancer using the Saos2 cell line. CRISPR software was used in an insilico study to identify the RNAs involved in osteosarcoma, specifically those of the control genes FGFR3P1 and CDK12.

Methods: Morphological characteristics of Ag NPs were analyzed from UV, SEM, and TEM. FTIR analysis was done to identify the functionalization of NPs.NPs showed excellent antibacterial effects against *S. aureus, L. monocytogenes, B. subtilis*, and *E. coli.* The DPPH assay indicates the level of inhibition increased with the rise in the concentrate of the sample. Invitro-anticancer and cell toxicity of biosynthesized Ag NPs against Saos2 (osteosarcoma) human bone cancer cell lines compared to normal cells were premeditated. The gene knockout mechanism was also explored by the CRISPR spcas 9 tool.

Results: Cell line studies conclude the level of cell viability of non-malignant growth cells gets diminishes as the concentration of phytosome increases. The CRISPR spcas9 genome editing software was utilized as an insilico approach to validate the efficacy of phytosome in the Saos2 (osteosarcoma) human bone cancer cell line, providing the gene knockout possibilities in cancer eradication.

Conclusion: The outcome from the exploration demonstrates phytosome was a good method for drug delivery with better value for bone malignant growth treatment. Besides, the CRISPR tool identified gene knock-out possibilities of control gene FGFR3P1 & CDK12 will pave the way for further research for treating human bone cancer.

Keywords: Antibacterial; Osteosarcoma; Phytosome; Insilico; CRISPR spcas 9; FGFR3P1; CDK12; Saos2 Cell line.

1. Introduction

In recent years, many synthesis approaches for nanomaterials have stayed a fascinating zone in nanoscience and technology. Green synthesis approaches are obtaining incredible consideration in existing research and improvement on technology and era. On the whole, green synthesis of nanomaterials, which was formed through guidelines, control, and remediation method, will be a tool in dealing with different illnesses. In the field of biotechnology, nanotechnology shows a vital part in allocating with synthesis, proposal, and manipulation of molecule arrangement differing from about 1-100 nm (Dubey D et al. 2007). Because of their exceptional properties like figure, size, antimicrobial and electrical properties, it became content for the scientists in the creation of silver nanoparticles. Applications of nanoparticles in sections such as biomedical, space research, optical science, health care, food technology, and photo-electrochemical applications are noted. Copious methods are involved in synthesizing nanoparticles. In the current report, the green synthesis of NPs is enhanced since chemical synthesis involves toxic chemicals which cause harm to the environment. Green synthesis of nanoparticles involves ecofriendly byproducts and non-toxic protocols which also lead to awareness in increasing the synthesis in biological approach. The green synthesis also has the advantage for chemical and physical techniques such as cost-efficient, eco-friendly, fewer usages of pressure, energy, and temperature (Mahendiran D et al. 2017). It is also scaled up for huge scale synthesis. Among numerous green production methods plant, intermediated synthesis comes out to be a positive method as it forms a stable nanoparticle in less time. This plant, which holds medicinal values with numerous therapeutic values forms the best podium for the production of nanoparticles that are also non-toxic and also offer natural covering agents. A wide variety of inorganic nanoparticles are presently used in biological applications because of their characteristic features such as non-toxic, hydrophilic, biocompatibility, wide availability, and ability of embattled medicine transport. Among various inorganic nanoparticles, silver nanoparticles have an exceptional belonging applied to antimicrobial effects, biosensor applications, cosmetic products, and optical probes.

The main problem in the conventional medicine delivery system is the limited allowance of the drug into the cells. To find a solution a carrier system has been chosen to improve efficiency in drug delivery. Phytosome also called the synergistic complex is a combination of herbal extract bounded with a lipid layer that acts as a carrier which helps in improving drug delivery at the site of infection. The layer above the extract protects the treasured elements that are available in the extract from the intestinal secretion and gut bacteria (Kumari P et al. 2011; Srikanth V et al. 2011).

These techniques illustrations more efficacies in the fascination of medication than the normal herbal extract. In this current study, plant extracts are chosen in such a way that and they are environmentally friendly and can investigate silver nanoparticle production. *Allium sativum* (garlic) has antibiotic, anti-tumor, and cholesterol-lowering properties. *Curcuma longa* (turmeric) has anti-inflammatory, anti-bacterial, anti-fungal, and antioxidant properties. *Murraya koeinji* (curry leaves) has antioxidant, wound healing, and fat lowering properties. The present-day study was approached in synthesizing silver nanoparticles from the garlic, turmeric, and curry leave aqueous extract. Phytochemical analysis was done for the sample extracts in ascertaining the bioactive components of the samples and their therapeutic values. Spectroscopic studies were done in evaluating the structure, morphology, and particle dimension of the manufactured silver nanoparticles. The prepared synergistic complex was tested against the tumor cells (Saos2) for its effectiveness against cancer diseases and the profile of continuous medication release was also investigated.

2. Materials and Approaches

2.1 Preparation Of Sample

M. koeinji, *A. sativum* and *C. longa* from Green Grow Cultivation Unit, Big Shop, Udhagamandalam, Tamil Nadu (preserved in a hygienic, sterilized pliable sealed container) and the authentication was done by Dr. Annamalai, Plant Biologist, Coimbatore and the voucher specimen (BIT/BT/MAC0519/2019) were deposited in Department of Biotechnology, Bannari Amman Institute of Technology Sathyamangalam, India. Herbs were washed, fragmented, and finally dried out in the oven at 38 °C for 5 hours. Each 10 g, were weighed, dissolved into 100 mL of purified water, and made to boil at 100°C for 15 minutes. Then, filtration was done. The extract was used for further analysis.

2.2 Production Of Ag NPs

In the beginning, 0.1M of silver nitrate was prepared for 100ml. Place the prepared silver nitrate in the magnetic stirrer. To that, add the prepared extract dropwise until color fluctuations happen. The centrifuge was done at 10,000 rpm for 900 seconds (Elshawy O.E et al. 2016). Then, the formed pellet was collected and well-kept in a hot air oven. Silver nanoparticles were scraped and stored.

2.3 Biosynthesized Silver Nanoparticles Characterization

Generally, the depiction of the particle is actualized by UV–Vis spectroscopy. The Ag NPs synthesized by bio-based route were checked by UV–Vis spectrophotometer (SL 171). An Equinox 3000 diffractometer was used for X-Ray Diffraction investigations of silver nanoparticles. Moreover, biosynthesized Ag NPs were perceived through SEM (SEM, HITACHI, and S-4160) and Transmission Electron Microscopy (TEM).

The size of Ag NPs utilizing Dynamic Light Scattering Malvern-Zetasizer (Nano-z 590) was analyzed (Naik R.R et al. 2002). FT-IR analysis was undergone to analyze the functionalizing group that presents in the herb that was a reason for the reduction of Ag ion, so the dried pellet of the extract from the sample of Ag NPs with KBr (1:100) which were utilized for FTIR spectrum examination of the Ag NPs prepared by the bio-based route.

2.3.1 UV–Vis Analysis of Biosynthesized Ag NPs

Different concentration of silver nitrate is prepared.5ml of the combined extract was added to the prepared solution of AgNO3 at various concentrations respectively. Then the absorbance values of each are noted when subjected to a UV spectrometer for multiple wavelengths ranging between 300-800 mm (Naik R.R et al. 2002; Gurunathan S et al. 2009). These mixtures are then incubated at room temperature for 24 hours in the dark. After another overnight incubation, the solutions are examined with a UV spectrometer and absorbance values are compared.

2.3.2 Scanning Electron Microscopy

The microstructure was examined by high-resolution Scanning Electron Microscopy (SEM; instrument from Nikon, Japan). To sum up things, Ag NPs were floated in ion-free H2O at centralization of 1 mg mL-1 and later were subjected to sonication till the extract homogenous suspension was formed (Joshi M et al. 2008). Afterward, a droplet of solicited fluid was dripped and dried on the glass plate. Later, it was coated with gold, and pictures were recorded. Scanning Electron Microscopy was utilized to portray the morphology and size of Ag NPs.

2.3.3 Transmission Electron Microscopy

The microstructure and size were analyzed by high-resolution TEM in a JEOL 3010, Japan, working at 200 kV as indicated by a method of with certain adjustments. In the short-term, Ag NPs (1 mg mL-1) were made floated in ion-free water then the extract was sonicated to make a homogenous suspension. For size estimation, the above fluid of NPs (0.5 mg/mL) was made 20 times dilution. TEM was done to describe the size and figure of the Ag NPs (Prashant Tiwari et al. 2011). A droplet of Ag NPs was dripped on a carbon-covered Cu grid and dried to get TEM pictures.

2.3.4 X-Ray Diffraction Study

The solid-state scatterings of silver nanoparticles were assessed with X-ray powder diffraction. Diffraction designs got utilizing a XPERT-Professional diffractometer (PA Nalytical Ltd., the Netherlands) with a range of 240 mm (Gurunathan S et al. 2009). A method of diverge and receiving slits of 1 and 0.1 mm was utilized. The prototype was collected with 40 kV of tube current and 30 mA of tube voltage and looked more than the 2 h scope of 10–90.

2.3.5 FTIR Analysis

The quantitative and qualitative analysis for natural and inorganic samples changed into evaluation with the assistance of FTIR. It generates an infrared absorption spectrum that reveals the identity of chemical bonds in a molecule. The spectra generate a pattern profile, a unique molecular fingerprint that may be used to screen and test samples for a variety of amazing additives. FTIR is a useful analytical technique for the popularity of purposeful businesses and characterizing covalent bonding statistics (Manopriya M et al. 2011). Initially, the pattern is exposed to multiple wavelengths of infrared light, and the device measures which wavelengths are absorbed. They were takings the fresh preoccupation statistics and conducting a math path called the Fourier Transform to deliver an understandable absorbance spectrum. This spectrum can then be associated with a library of spectra to find a suit.

2.4 Antibacterial Assay of Biosynthesize Ag NPs

2.4.1 Agar Well Diffusion Method

The antibacterial evaluation was primarily trailed through Agar well diffusion and disc diffusion technique. In this enterprise, we accompanied the Agar-well diffusion method. The antibacterial assay was done against four bacterial cultures namely *Escherichia coli* (1687), *Listeria monocytogenes* (657), *Staphylococcus aureus* (737), and *Bacillus subtilis* (441). Initially, we took sterilized Petri plates and swabs (Bala N et al. 2015). The nutrient agar was prepared in decontaminated Erlenmeyer flask and was sterilized at 121 ºC for 15 minutes. Transfer the nutrient agar into the sterilized plate and leave it undisturbed until it gets solidified. The culture was swabbed in the plate. Once swabbing is completed, a well was made on the plate. The sample at altered concentration was added to the well, was kept back undisturbed in the incubator at 370 ºC for 24 - 48 hours (Vignesh V et al. 2013). The zone of inhibition for the individual concentration was measured which was formed on the plate.

2.5 Synthesis Of Synergistic Emulsion

Synergistic Emulsion was prepared by combining phospholipids with the biosynthesized Ag NPs in 1:1 proportion through consistent stirring. At that point, the compound was heated to 65°C in a hot air oven for evacuation of the solvent (Kirby C.J and Gregoriadis G 1984). The subsequent suspension of Phytosomal was stored at 20 to 22 ˚C.

2.6 Characterization Of Synergistic Emulsion

2.6.1 Scanning Electron Microscopy

Characterization of phytosome is done by SEM technique. The outer structure of the phytosome be analyzed by SEM recording (JEOL-MODLE 6390) at 20KV.

2.6.2 Entrapment Efficiency

Centrifugation (45 minutes) of the emulsion was done at 15000 rpm to isolate the collegial substance as free medication (Sharma A and Sharma U.S 1997). The drug quantity in the supernatant was estimated by recording A217. The level of medicine entrapment was determined utilizing the equation.

2.6.3 In Vitro Drug Release Study

Collegial emulsion synthesized weighing a measure of 1 gram was included into a container containing 150 ml of pH 7.4 PBS. The prepared emulsion was mixed in a magnetic stirrer (300 rpm, 37 ˚C) (Srikanth V et al. 2011). At regular periods, emulsion (3 mL) was taken back and compensation was made with fresh PBS immediately (Acharya N.S et al. 2011). A217 was recorded, and then the rate of release of the drug was determined.

2.6.4 Release Kinetics

Release kinetics of emulsion contain 0.5~10%, synergistic biosynthesized silver nanoparticles with phospholipid was investigated using the Korsmeyer-Peppas equation, where the linear regression of Log (Mt/M) versus Log(t) arc shows the phytosome release model. The first 60% of drug release data were fitted in the Korsmeyer-Peppas model,

$F = (Mt/M) = Km\ tn$

where F, Km, M, Mt, t, n is drug released fraction at the time 't', Kinetic constant, the total amount of medicine in dose form, rate of drug released at the time 't', time in hours, and diffusion or release exponent respectively.

Note that 'n' can be predicted using linear regression of log (Mt/M) versus log(t)

2.7 Antioxidant Activity

The antioxidant activity of the consolidated extract was assessed using the effect on the constant DPPH free radical, with the work solution consisting of various concentrations (0.5, 1, 1.5, 2, and 2.5 mg/ml) (Nenadis N et al. 2004). Using the equation, the level of DPPH inhibition was estimated.

Where AS and AC are test sample and control absorbance respectively.

2.8 Anticancer Study Of Biosynthesized Ag NPs

In-vitro cytotoxicity assay and anticancer activity on Saos2 cell line

MTT (Methylthiazol Tatrazolium) assay was used to calculate the viable cells.

2.8.1. Cell Culture

Saos2 cell lines were treated with MEM medium with fetal bovine serum. The cells were kept under optimal conditions, with a CO2 concentration of 5% and a temperature of 37°C. To ensure cell viability, the medium was altered every three days.

2.8.2. MTT Assay

In vitro cytotoxicity of biosynthesized nanoemulsion / phytosome was determined using MMT assay. Different types of extract solutions were made as follows: 1. Direct extract, 2. Extract with PBS, 3. Extract with cottonseed oil. Different concentrations of extracts were treated with Saos2 cells in 96 well plates and kept for 24 hours (Omar S.H and Al-Wabel N.A 2010). MTT solution was prepared using PBS in the (5 mg/mL). Each well was augmented with MTT solution and kept for 4 hours of incubation. The media was replaced with 150 µl of DMSO and followed by recording A540 with an ELISA reader.

2.8.3. Cell Viability Assay In Treating Bone Cancer

Bacterial cell viability was determined using the 3-(4,5 dimethylthiazol-2-yl)-2,5-diphenyltetrazolium bromide (MTT) technique after 12 hours of dealing with silver nanoparticles, as directed by the standard procedure (Taiichiro Seki et al. 2008). Centrifugation (1000g, 10 min) of drug-treated Saos2cell line culture was done at 4 ºC and continued to wash multiple times with germ-free pH 7.4 PBS. Then, replaced medium with a new RPMI (with no FBS and phenol red) containing MTT (0.5 mg mL-1). After extra 3 hours of incubation at 37 ºC, HCl – isopropanol mixture gets included, 15 minutes of incubation at 37 ˚C, solubilized MTT formazan product absorbance was calculated at 570 nm.

2.9 Apoptosis Assay

The analysis of the apoptotic effect of the collegial emulsion on Saos2 osteosarcoma cells with the aid of assay of DNA fragmentation and nuclear DNA staining was performed. In nuclear DNA staining, paraformaldehyde (4%) in PBS was applied to fix compound-handled and control cells for 20 mins and PBS washing was done. Then, 1 mg mL-1 Hoechst 33258 in PBS was used to stain for 15 minutes. 2× PBS washing was performed for stained cells. A fluorescent microscope (Olympus, Melville, NY) with a UV filter was used to see the nucleus modification. In the assay of DNA fragmentation, each indifferent and connected compound-treated or control cells harvesting was done by centrifuge and scraping techniques. The lysis buffer (Triton X-100 (0.5%), pH 8 Tris (5 mM) EDTA (20 mM)) was applied to lyse the cells on ice (45 minutes) (Leung D.Y 2000). Extraction of fragmented DNA using 2× chloroform: phenol: isoamyl alcohol (24:25:1, v/v) from centrifuged (14,000 rpm, 45 mins, 4°C) supernatant and later triggered using sodium acetate (3 M) and ethanol for an in a single day at −20°C. Ethanol (70%) was used and washing of DNA pellet was performed. Then suspended in pH 8 Tris-EDTA buffer containing RNase (100 µg mL-1) and kept incubated (37 °C, 2 h). Agarose gel electrophoresis (1.8%) was applied to separated DNA fragments and monitored beneath UV light.

2.10 Western Blot Analysis

In a 10 cm dish, Saos2 Osteosarcoma cells were cultivated. After 80–90% confluence of cell density attainment, cells had been exposed to collegial emulsion (500 μg mL-1) for mentioned times. The ice-bloodless PBS was used for washing of cells and lysis buffer (20% SDS with sodium fluoride (5mM), sodium orthovanadate (0.1 mM), antipain (1 mM), iodoacetamide (10 mM), leupeptin (1 mM), phenylmethylsulfonyl fluoride (2 mM)) was applied to lyse cells (10–20 minutes). The sonication of lysates at 10-sec intervals was done, aliquots were taken and saved at −20 °C. The Bio-Rad DC protein test (Bio-Rad Laboratories, Hercules, and CA) is used to estimate protein awareness. The same amount of protein (20 g lane-1) was loaded onto a 12 percent SDS-PAGE and transferred to a nitrocellulose membrane (Leung D.Y 2000). The membrane was kept incubated with the following antibodies: a rabbit anticaspase7 polyclonal antibody; a mouse anti-PARP monoclonal antibody; a mouse anti-E2F1 monoclonal antibody; a rabbit anti-cdk4 polyclonal antibody; a mouse anti-cyclin D1 antibody; a rabbit anti-Bax antibody; a mouse anti-p53 monoclonal antibody; a mouse anti-Bcl2 monoclonal antibody; a rabbit anti-p21Cip1/WAF1 polyclonal antibody was acquired from Chemicon International Inc. (Temecula, CA), Santa Cruz Biotechnology (Santa Cruz, CA), Sigma, Zymed Laboratories Inc. (South San Francisco, CA) respectively. Antibody recognition is detected using a secondary antibody, either antirabbit IgG or anti-mouse IgG, in combination with horseradish peroxidase (Zymed). The ECL Western blotting evaluation tool had recognized antibody-specific proteins (Amersham Pharmacia Biotech, UK).

2.11 Statistical Analysis

The software was also used to analyze the transcription system of osteosarcoma. The method began by examining the primary sequence in order to identify the early coding region, which was followed by the identification of possible targets. The azimuth score achieved by each gene was calculated by comparing these targets to the 278627679 sites. Finally, suitable RNAs for gene knockout were selected.

3. Result And Discussion

3.1 Biosynthesis of Ag NPs

The fresh extracts of *M. koeinji*, *A. sativum*, and *C. longa* were initially yellowish-green in color. A few drops of silver nitrate solution were added to that solution and were kept rousing at 20 ºC until the solution color changes into reddish brown which was shown in Supplementary Figure S1a. The simple chemistry behind this was the increased color intensity confirms the reduction activity of Ag ions and Ag NPs formation. The primary evidence to be noted for the occurrence of Ag NPs was the surface plasmon excitation which was responsible for the change of color. The EDX spectrum of the prepared Ag nanoparticles is shown in Figure 1c. The Silver (Ag) signal comes from Ag nanoparticles, with a 31.39 percent atomic percentage of Silver.

Carbon, chlorine, oxygen, and sodium were among the other peaks discovered. Other elements, with the exception of carbon, have a very low atomic percentage as compared to Silver, implying the production of pure Ag NPs.

Different peaks at 2θ values in Ag NPs pattern can be legitimate to the deposits of the natural substance material of the blended concentrate (Joshi M et al. 2008). These peaks show the crystallization of few sample metabolite moieties at the external side of the Ag NPs. This is a reasonable proof to confirm the inclusion of the joined concentrate arrangements inside the Ag NP development.

3.2. Biosynthesized Ag NPs Characterization

3.2.1 UV–Vis Analysis of Biosynthesized Ag NPs

The ultraviolet-visible absorption range of Ag NPs is shown in Supplementary Figure S1b. From UV–Vis assessment range of Broad chime molded bend was acquired. Different metabolites from *M. koeinji, A. sativum* and *C. longa* extract acquainted with arrangement make the plasmon band wide for the reason which it might be read in that particular absorption range. The sample demonstrated the trait surface-plasmon (Joshi M et al. 2008). The most extreme band was seen at 415 nm. The greatest peak in the retention range of triangular Ag NPs was found approximately between 420 and 450 nm in range, with a blue or red shift when molecule size decreased or expanded, respectively.

3.2.2 SEM Analysis

Scanning electron microscopy is keen on analyzing the dimension, figure and morphological characteristics features of ecofriendly biosynthesized silver nanoparticles (Prashant Tiwari et al. 2011). The individual Ag NPs are clearly shown in Figure 1a. From the image, we could also depict that they are triangular.

3.2.3 Transmission Electron Microscopy

The TEM results confirm the Ag NPs are triangular in shape and size ranges with a mean span of 16 ± 2 nm. From (Figure 1b) it was demonstrated that Ag NPs have not no physical contact with each other and was evenly distributed. It was likewise seen that Ag NPs were uniformly dispersed

3.2.4 X-Ray Diffraction Analysis

XRD test discovered discrete peaks at 2θ values, which might be ascribed to 111, 200, 220 and 311 crystalline planes of Ag NPs is shown in Figure 1d. These peaks are related with the face centered cubic grid.

3.2.5 FTIR Analysis

FTIR analysis was done primarily to analyze the structural and functional knowledge about the macromolecule. FTIR spectrum (Figure 1e) recorded shows shift in peaks from 3570-3200 (due to OH stretch and polymeric OH stretch), 2935- 2915 (due to methylene C-H asymmetry stretching), 2880-2860 (due to methyl C-H asymmetry/symmetry stretch), 1650-1590 (corresponding primary amine NH lend) this particular absorption peak that proteins had been cooperated NPs prepared in bio-based route and their 2° structure become unaffected sooner or later of response with Ag+ particles or after binding with Ag NPs, 1650-1550 (imino compound NH-stretch), 1350-1260 (corresponding phenol or tertiary group), 1150-1050 (alkyl-substituted ether C-O stretch), 1190-1130 (due to CN stretch secondary amine), 1150-1050 (alkyl-substituted ether C-O stretch), 500-470 (due to S-S stretch polysulphsider and aryl disulfides S-S stretch). FTIR is a useful analytical technique for the popularity of purposeful businesses and characterizing covalent bonding statistics (Manopriya M et al. 2011). Initially, the pattern is exposed to multiple wavelengths of infrared light, and the device measures which wavelengths are absorbed. They were takings the fresh preoccupation statistics and conducting a math path called the Fourier Transform to deliver an understandable absorbance spectrum. This spectrum can then be associated with a library of spectra to find a suit.The FTIR estimations of green blended Ag NPs were done to distinguish the conceivable cooperation between protein and Ag NPs (Manopriya M et al. 2011). The result obtained indicates that the presence of some proteins can be act as stabilizing and reducing agents.

3.3 Antibacterial Activity

The examination of antibacterial activity showed that the sample had antibacterial activity among different categories of bacterial species namely *S. aureus*, *L. monocytogenes*, *E. coli*, and *B. subtilis* (S2).

3.4 Synergistic Emulsion Study:

The synergistic emulsion was prepared by the combination of phospholipid and biosynthesized Ag NPs 1:1 ratio. From certain reference papers, the perfect combination in preparing phytosome was observed to be a 1:1 ratio. Different combinations of phytosome liposomes and the plant extract were tested shows a result with a minimum efficiency of 32.80 ± 6.3%. These results revealed that the phytosome complex made out of biosynthesized Ag NPs has higher entrapment effectiveness than the liposome. These results revealed that the phytosome complex made out of biosynthesized Ag NPs has higher entrapment effectiveness than the liposome (Barenholz Y 2003).

Initially, there was 81.24 % of drug release for both biosynthesized Ag NPs phytosome complex and the combined extract (Acharya N.S et al. 2011). After every one hour, the drug release study was performed and there was a constant increase in the release of drugs to time (Srikanth V et al. 2011).

But the cumulative drug release for biosynthesized nanoemulsion/phytosome (74.63 %) was greater when compared with the drug release of the combined extract (53.89 %) which was depicted in the graph. from the results, we could infer that the drug release was time-dependent and reliable in drug dosage delivery treatment.

3.5 Characterization Of Synergistic Emulsion

3.5.1 SEM Analysis

The morphological view of the phytosome, which was assumed to be spherical, is depicted in the SEM image. From the supplementary figure S3, it was analyzed that the combined extract was trapped inside the phospholipid matrix (Kirby C.J and Gregoriadis G 1984). At 30,000x the size of biosynthesized Ag NPs encumbered in the phytosome complex was found to be 500nm (S3) The mean dimension of Ag NPs was noted as 18 ± 3 nm. The noted nanoparticle size (SEM and TEM) transformed into scarcely bigger than the hydrodynamic distance across acquired from the DLS explore. . This is because in the DLS experiment hydrated condition of the sample was estimated though in the TEM dried condition of the sample was estimated (Balamurughan M.G et al. 2014). The TEM picture uncovered that the nanoparticles had been inserted in a thick network which might be the regular settling added substances of those mixed concentrates.

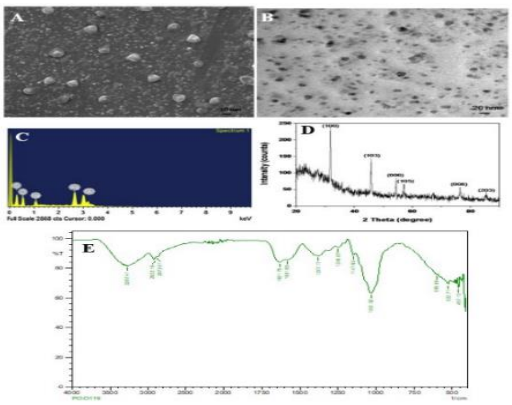

Figure 1: (a) Scanning electron microscopy, (b) Transmission electron microscopy, (c) Energy-dispersive X-Ray spectrum, (d) X-Ray diffraction, and (e) FT-IR spectra of biosynthesized Ag NPs

3.5.2 Entrapment Efficiency

The entrapment effectiveness of the synergistic combination of phospholipid-biosynthesized nanoparticles was found to be 95.80%. The phospholipid and the combined extract show more entrapment efficiency than any other complex this was proved from data collected from certain references related to the entrapment efficiency.

3.5.3 In Vitro Drug Release Study

The graph (figure 2a) explains the comparison of biosynthesized Ag NPs phytosome complex and herbal extract in drug release percentage in Phosphate Buffer Saline and phosphatidylcholine. The percentage drug release of the phytosome complex was better than the combined extract. At different time intervals, the drug release biosynthesized nanoemulsion / phytosome and the herbal extract were analyzed.

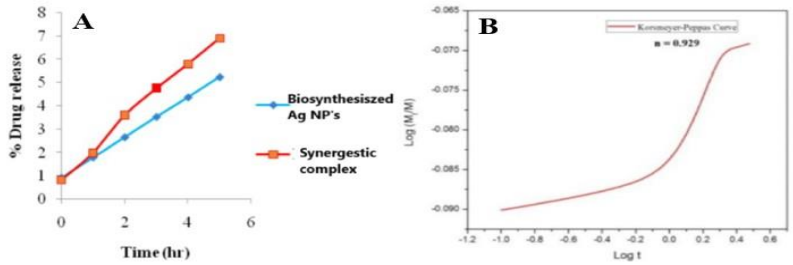

Figure 2: (a) Drug release comparison between biosynthesized Ag NPs and synergetic complex and **(b)** Korsmeyer Peppas curve of Log (Mt/M) Vs Log t

3.5.4 Release Kinetics

The release of the drug (figure 2b) was zero-order which can be confirmed from the 'n' value that is 0.929. It is autonomous of concentration and time subordinate. This demonstrates medicate discharge isn't influenced by the fixation slope for a certain timeframe and makes it a perfect method of medication conveyance. The results are compared with plant extract release kinetics. Phyllanthin from phytosome and the value of n range from 0.912 to 0.998 which correlates that the phytosome complex is suitable for the sustainable drug release of the biosynthesized Ag NPs.

3.6 Antioxidant Activity

The outcomes of cancer prevention agent action by utilizing the DPPH measure show that the rate restraint increments with increases in the centralization of the extract as demonstrated in figure 3a. Extract discharged from the synergistic complex has no physicochemical differentiation from the concentrate. Thus, antioxidant potency action of the synergistic complex for time has been delineated in figure 3b. The zone of inhibition formation concludes that the extract has strong antibacterial activity. (Sathishkumar M et al. 2010). The strongest antibacterial activity with the greatest zone of inhibition (21 mm) was recorded against the standard strain of *S. Aureus* (Supplementary figure S2).

Initially, we took sterilized Petri plates and swabs (Bala N et al. 2015). The nutrient agar was prepared in decontaminated Erlenmeyer flask and was sterilized at 121 ºC for 15 minutes. Transfer the nutrient agar into the sterilized plate and leave it undisturbed until it gets solidified.

The culture was swabbed in the plate. Once swabbing is completed, a well was made on the plate. The sample at altered concentration was added to the well, was kept back undisturbed in the incubator at 370 ºC for 24 - 48 hours (Vignesh V et al. 2013). The zone of inhibition for the individual concentration was measured which was formed on the plate.

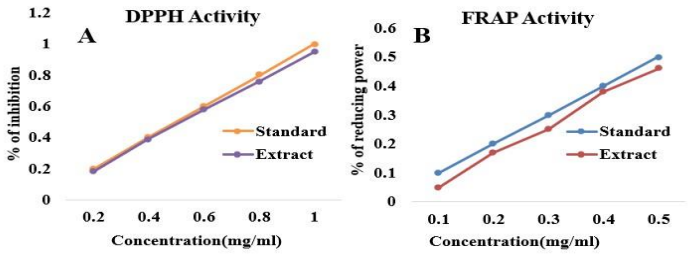

Figure 3: Antioxidant assay (a) DPPH activity and (b) FRAP activity

3.7 Anticancer Study of Biosynthesized Ag NPs

3.7.1 Cell Culture

An altered concentration of the biosynthesized nanoemulsion/phytosome was treatedwithSaos2 cells. After 24 hours, mild to severe cytotoxic reactivity was observed. The percentage of cell viability gets decreased to the concentration of biosynthesized nanoemulsion/phytosome. Control gave no cytotoxicity as expected. Distribution of cell cycle in Saos2osteosarcoma cells are exposed to the synergistic emulsion. The G1 phase quantity of cells improved steadily, and the S phase range of cells reduced notably from 12–48 hrs after exposure.

3.7.2 Cell Viability

From the results, it is concluded that the percentage of cell viability of non-cancer cells get decreased as the concentration of biosynthesized nanoemulsion /phytosome increases. No change was observed in the Cell viability of control cells.

3.7.3 MTT Assay

The MTT results showed that the sample extract has mild effects over the Saos 2 cancer cells. The cytotoxic activity of the biosynthesized nanoemulsion/phytosome of Saos 2 cells from osteosarcoma was investigated. The data indicated cell growth and viability reduction in a dose-dependent way. Saos2 cells treated with different concentrations were displayed in figure 4a. After 24 hours, mild to severe cytotoxic reactivity was observed. The percentage of cell viability gets decreased to the concentration of synergistic complex/phytosome. Cytotoxicity activity of biosynthesized nanoemulsion /phytosome was performed on Saos 2 cell lines at various concentrations to estimate the IC50 by MTT assay (Omar S.H and Al-Wabel N.A 2010; Taiichiro Seki et al. 2008). Outputs of various concentrations are tabulated (Table 1).

It was observed inhibition of growth (%) increased with the rise in concentrations of test compound, and the IC50 value was 37.25mg/ml.

Table 1: MTT Cytotoxicity assay

S.No	Concentration (µg/ml)	% of Cell Death	% of Live Cells
1	250	65.10	20.81
2	100	64.36	32.37
3	50	63.62	36.09
4	25	42.38	51.97
5	12.5	34.13	70.48
6	6.25	39.14	79.57
7	3.125	28.95	83.57
7	1.562	18.50	88.76
8	0.781	8.05	95.94

3.7.4 Apoptosis Assay

The apoptotic impact of the collegial emulsion onSaos2 osteosarcoma cells has been investigated by utilizing atomic DNA recoloring and DNA discontinuity examination (figure 4b). Acridine orange/propidium iodide (AO/PI) staining in combination with fluorescence microscopy was used to evaluate the morphology of Saos2 human osteosarcoma cells. For 48 hours, cells were treated with Biochanin A at concentrations of (A) 0, (B) 10, (C) 50, and (D) 100 M. Normal cells have green fluorescence, while apoptotic cells have orange/red fluorescence. (E) Apoptotic cell quantification * P0.05, ** P0.01, and *** P0.001 were regarded as statistically significant. Control and compound-treated cells were fixed in 4 percent paraformaldehyde in PBS for 20 minutes, washed with PBS, and recolored with Hoechst 33258 at 1 µg/ml in PBS for 15 minutes for atomic DNA recoloring. 2× with PBS was used to wash the recolored cells. The alterations in cores have been found with a luminous magnifying lens through UV-filter. For the DNA fracture test, each unconcerned and associated oversee or compound-treated cell was gathered with the guide of scratching and centrifugation. The cells were then lysed on ice for 45 minutes with lysis buffer (5 mM Tris [pH 8.0] 20 mM EDTA, 0.5 percent Triton X100). After centrifugation at 14,000 rpm for 45 minutes at 4°C, divided DNA inside the supernatant part was extracted 2× with phenol: chloroform: isoamyl liquor (25:24:1, v/v) and once with chloroform, then supported with ethanol and 3M sodium acetic acid derivation medium-term at 20°C. The DNA pellet is washed in 70% ethanol, then resuspended in a Tris EDTA cushion (pH 8.0) with a 100 g/ml RNase and brooded for 2 hours at 37°C. The DNA fragments were isolated using a 1.8 percent agarose gel electrophoresis and photographed under UV light.

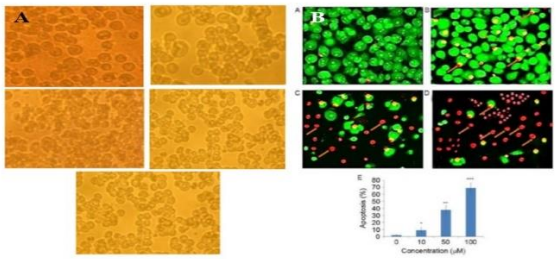

Figure 4: (a) Cytotoxicity effect of extract synergistic complex/phytosome contrary to Saos2 cell line and (b) Cytotoxicity analysis of Biosynthesized Ag NPs -Synergistic emulsion.

3.7.5 Western Blot Analysis

In a 10 cm dish, Saos2 Osteosarcoma cells were developed. Cells were treated with collegial emulsion (500 g/ml) for the showed occasions when cell thickness reached 80–90 percent intersection. The cells were then rinsed once in ice-cold PBS and lysed for 10–20 minutes with lysis support (20 percent SDS with 2 mM phenylmethylsulfonyl fluoride, 10 mM iodoacetamide, 1 mM leupeptin, 1 m Mantipain, 0.1 mM sodium orthovanadate, and 5 mM sodium fluoride). The lysates were sonicated 3× at 10-second intervals, aliquoted, and stored at 20°C. The Bio-Rad DC protein examination was used to fix the protein issue (Leung D.Y 2000). Equivalent amounts of protein (20g/path) were exposed on a 12 percent SDS-PAGE and transferred to a nitrocellulose layer.

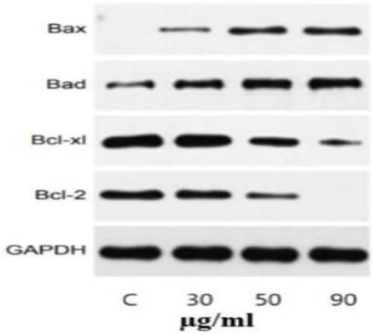

Figure 5: Western blot analysis of caspase-3 and caspase-8 expression in Saos2 cells.

The layers were then end brooded with the appropriate number one antibodies, as shown: a hare antip21Cip1/WAF1 polyclonal immune response, a mouse antiBcl2 monoclonal counter acting agent; a mouse antip53 monoclonal immunizer, a bunny anti-Bax neutralizer (Sigma); a mouse anti-cyclin D1 immunizer, a hare anticdk4 polyclonal counteracting agent, a mouse anti-E2F-1 monoclonal counter acting agent, a mouse anti-PARP monoclonal immune response; a hare anti-caspase-7 polyclonal immunizer. Immunizer acknowledgment became distinct with the addition of a separate auxiliary counteracting agent, either anti-mouse IgG or anti-rabbit IgG antibodies in combination with horseradish peroxidase (Zymed). The ECL western smudging examination framework was used to differentiate antibody-sure proteins.

Western blot analysis was used to look at the levels of caspase-3 and caspase-8. In the combined group (extract was 140 L/mL and cisplatin was 6 g/mL), active caspase-3, PARP, and active caspase-8 all increased are shown in (figure 5).

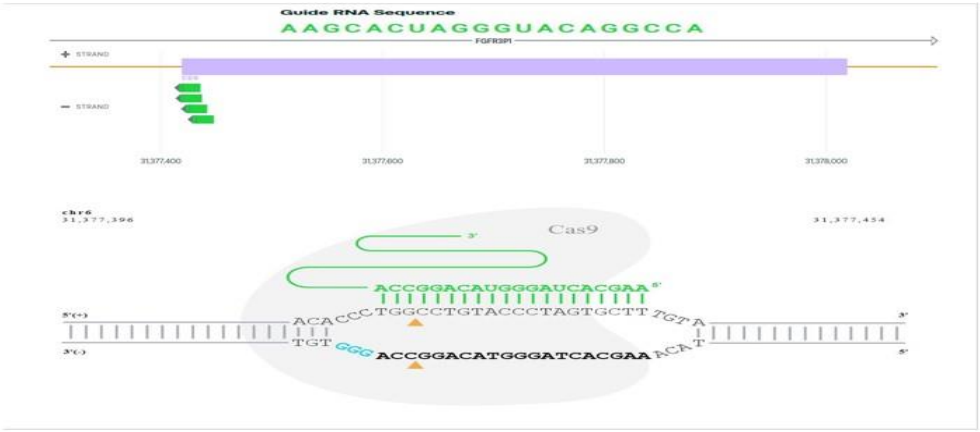

Figure 6: CRISPR-SpCas9 predicted a gene knockout sequence for *Homo sapiens*. The role of RNA splicing in reversing the FGFR3P1 function is indicated.

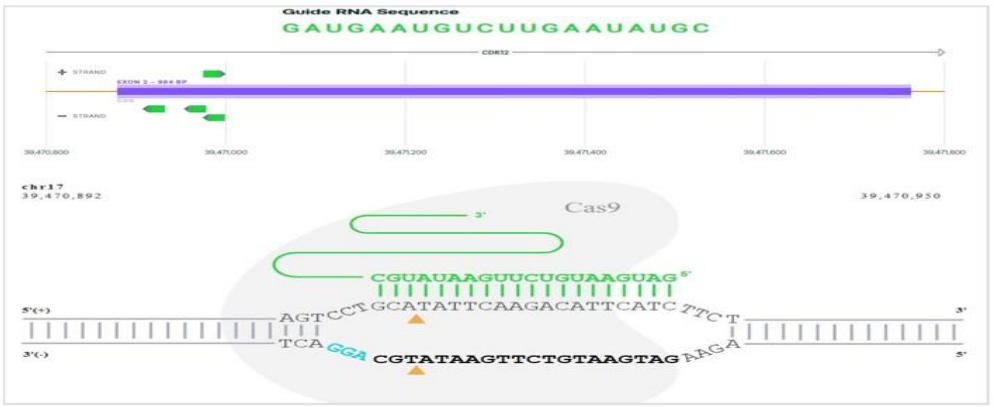

Figure 7: CRISPR-SpCas9 predicted a gene knockout sequence for *Homo sapiens*. The role of RNA splicing in reversing the CDK12 function is indicated.

3.8 In Vitro Analysis Of Gene Expression Using Crispr

CRISPR spcas9 was utilized in genome engineering CRISPR software to validate the gene knock out of FGFR3P1, CDK12 in the Homo sapiens Saos2 (Osteosarcoma) cell line. For the probable regulator FGFR3P1, CDK12, the results were obtained. The CRISPR spcas9 editing tool was used to investigate the possibility of knocking out this gene in vitro because it controls the complete metabolism of transcription factors in osteosarcoma. The anticancerous characteristics were identified and validated using an insilico technique and recommend RNAs for gene knockout to inhibit osteosarcoma exhibited by the transcription gene FGFR3P1,

CDK12 (Figure 6 and Figure 7). In humans, the exon base for excision begins around 12379300bp. As a result, it is clear that human metabolism is confirming clinical trials. This structure has recently gained a lot of attention as a feasible and basic genome-designing device, and it has transformed the current sciences. It has been recognized for its potentially transformative applications in transcriptional irritability, epigenetic regulation, base changing, high-throughput heredity screening, and disease models in animals or cells. The use of genomic alterations to address infection-causing mutations is a promising strategy for treating human maladies. The bunched consistently interspaced short palindromic rehashes (CRISPR) /CRISPR-related protein 9 (Cas9) frameworks have greatly improved the capacity to roll out precise advancements in the human genome as a fundamental and programmable nuclease-based genomic modifying instrument. CRISPR-based improvements have recently improved at a rapid pace, broadening their application area and progressing CRISPR-based medications in preclinical trials. The advancement and application of the CRISPR framework in base altering, interpretation tweak and epigenetic changing, genomic-scale screening, and cell and incipient organism therapy in the last two years. Finally, the opportunities and steps identified with the use of CRISPR/Cas9 advancements.

4. Acknowledgement

This is the B.Tech final year project of first , second , third and fourth author .We acknowledge Department of Biotechnology , Sri Shakthi Institute Of Engineering And Technology for providing an ambient environment for the completion of project.

5. Conclusion

The aqueous extracts of garlic, turmeric, and curry leaves were used to synthesize silver nanoparticles. FTIR, SEM, TEM, and XRD were used to characterize the silver nanoparticles. Phytosome prepared through interaction among phospholipid and the blended extract. This property which is additionally answerable for hostile to malignant growth action has been affirmed. The IC50 esteem was recognized to be 37.25μg/ml. This demonstrates that the combined concentrate epitomized in phytosome can be the best approach of drug delivery with an upgraded incentive for the treatment of bone malignancy. The CRISPR spcas9 software was used to perform an in-silico study and gene knockout mechanism to discover the RNAs involved in osteosarcoma, particularly those of the regulatory genes FGFR3P1 and CDK12, for further research into treating human bone cancer. Numerous zones are to be investigated in the future to perceive the pharmaceutical applications.

6. Declarations:

Conflict of interest: The authors report no conflicts of interest.

Funding: The Source of funding is nil.

Ethical Clearance: Nil.

Permission To Reproduce: Nil.

7. References:

Acharya, N. S., G. V. Parihar, and S. R. Acharya. "Phytosomes: Novel approach for delivering herbal extract with improved bioavailability." *Pharma science monitor* 2, no. 1 (2011): 144-160..

Aniket, Kumari A, Kumari P, Saurabh S, Khurana L, Rathore K.S (2015Aniket, A., P. Kumari, S. Kumari, L. Saurabh, K. Khurana, and S. Rathore. "Formulation and evaluation of topical soy-phytosome cream." *Indian journal of Pharmacy and Pharmacology* 2, no. 2 (2015): 105-112.. Indian Journal of Pharmacy and Pharmacology ISSN: 2393-9087 2(2):105-112.

Bala, Niranjan, S. Saha, M. Chakraborty, M. Maiti, S. Das, R. Basu, and P. Nandy. "Green synthesis of zinc oxide nanoparticles using Hibiscus subdariffa leaf extract: effect of temperature on synthesis, anti-bacterial activity and anti-diabetic activity." *RSC Advances* 5, no. 7 (2015): 4993-5003.

Balamurughan M.G, Mohanraj S, Kodhaiyolii S, Pugalenthi V (2014) *Ocimum sanctum* leaf extract mediated green synthesis of iron oxide nanoparticles: spectroscopic and microscopic studies. Journal of Chemical and Pharmaceutical Sciences ISSN: 0974-2115 (4):201-204.

Barenholz, Yechezkel. "Relevancy of drug loading to liposomal formulation therapeutic efficacy." *Journal of liposome research* 13, no. 1 (2003): 1-8.

Dubey, D., S. Shrivastava, S. Kapoor, and P. K. Dubey. "Phytosome: a novel dosage structure." *Pharmaceutical Review* (2007): 1-8..

Elshawy, Omama E., Eman A. Helmy, and Laila A. Rashed. "Preparation, characterization and in vitro evaluation of the antitumor activity of the biologically synthesized silver nanoparticles." *Advances in Nanoparticles* 5, no. 02 (2016): 149-166.Gurunathan S, Kalishwaralal K, Vaidyanathan R, Venkataraman D, Gurunathan, Sangiliyandi, Kalimuthu Kalishwaralal, Ramanathan Vaidyanathan, Deepak Venkataraman, Sureshbabu Ram Kumar Pandian, Jeyaraj Muniyandi, Nellaiah Hariharan, and Soo Hyun Eom. "Biosynthesis, purification and characterization of silver nanoparticles using Escherichia coli." *Colloids and Surfaces B: Biointerfaces* 74, no. 1 (2009): 328-335.

Jayaprakasha, Guddadarangavvanahally Krishanareddy, L. Jaganmohan Rao, and Kunnumpurath K. Sakariah. "Antioxidant activities of curcumin, demethoxycurcumin and bisdemethoxycurcumin." *Food chemistry* 98, no. 4 (2006): 720-724.

Joshi, Mangala, Amitava Bhattacharyya, and S. Wazed Ali. "Characterization techniques for nanotechnology applications in textiles." (2008).

Keerthi, B., Prasuna Sundari Pingali, and Prathima Srinivas. "Formulation and evaluation of capsules of ashwagandha phytosomes." *Int J Pharm Sci Rev Res* 29, no. 2 (2014): 138-142.

Kidd, Parris, and Kathleen Head. "A review of the bioavailability and clinical efficacy of milk thistle phytosome: a silybin-phosphatidylcholine complex (Siliphos)." *Alternative Medicine Review* 10, no. 3 (2005).

Kirby, Christopher J., and Gregory Gregoriadis. "A simple procedure for preparing liposomes capable of high encapsulation efficiency under mild conditions." In *Liposome technology*, pp. 19-27. CRC Press, 2019.

Kumari, Parveen, N. Singh, and B. P. Cheriyan. "Neelam, Phytosome: A Noval Approach For Phytomedicine." *International Journal of Institutional Pharmacy and Life Sciences* 1, no. 2 (2011).

Leung, Donald YM. "Atopic dermatitis: new insights and opportunities for therapeutic intervention." *Journal of Allergy and Clinical Immunology* 105, no. 5 (2000): 860-876.

Mahendiran, D., G. Subash, D. Arumai Selvan, Dilaveez Rehana, Raju Senthil Kumar, and A. Kalilur Rahiman. "Biosynthesis of zinc oxide nanoparticles using plant extracts of Aloe vera and Hibiscus sabdariffa: phytochemical, antibacterial, antioxidant and anti-proliferative studies." *BioNanoScience* 7 (2017): 530-545.

Priya, M. Mano, B. Karunai Selvi, and J. A. Paul. "Green synthesis of silver nanoparticles from the leaf extracts of Euphorbia hirta and Nerium indicum." *Digest Journal of Nanomaterials & Biostructures (DJNB)* 6, no. 2 (2011).

Mauri, Pierluigi, Paolo Simonetti, Claudio Gardana, Markus Minoggio, Paolo Morazzoni, Ezio Bombardelli, and Piergiorgio Pietta. "Liquid chromatography/atmospheric pressure chemical ionization mass spectrometry of terpene lactones in plasma of volunteers dosed with Ginkgo biloba L. extracts." *Rapid Communications in Mass Spectrometry* 15, no. 12 (2001): 929-934.

Naik, Rajesh R., Sarah J. Stringer, Gunjan Agarwal, Sharon E. Jones, and Morley O. Stone. "Biomimetic synthesis and patterning of silver nanoparticles." *Nature materials* 1, no. 3 (2002): 169-172.

Nenadis, Nikolaos, Lan-Fen Wang, Maria Tsimidou, and Hong-Yu Zhang. "Estimation of scavenging activity of phenolic compounds using the ABTS•+ assay." *Journal of agricultural and food chemistry* 52, no. 15 (2004): 4669-4674.

Omar, Samar Hinkson, and N. A. Al-Wabel. "Organosulfur compounds and possible mechanism of garlic in cancer." *Saudi Pharmaceutical Journal* 18, no. 1 (2010): 51-58.

Kumar, Mandeep Kaur, Gurpreet Kaur, and Harleen Kaur. "INTERNATIONALE PHARMACEUTICA SCIENCIA." (2011).

Sathishkumar, Muthuswamy, Krishnamurthy Sneha, and Yeoung-Sang Yun. "Immobilization of silver nanoparticles synthesized using Curcuma longa tuber powder and extract on cotton cloth for bactericidal activity." *Bioresource technology* 101, no. 20 (2010): 7958-7965.

Sharma, Amarnath, and Uma S. Sharma. "Liposomes in drug delivery: progress and limitations." *International journal of pharmaceutics* 154, no. 2 (1997): 123-140.

Sricanth, V., C. Laxmaiah, B. Shankar, P. Naveen, B. Chiranjeeb, and T. Shivaraj Gouda. "Phytosome a novel drug system for improving bioavailability of herbal medicine." *Int J Pharm Res Dev* 3 (2011): 175-184. Seki, Taiichiro, Takashi Hosono, Tomomi Hosono-Fukao, Kahoru Inada, Rie Tanaka, Jun Ogihara, and Toyohiko Ariga. "Anticancer effects of diallyl trisulfide derived from garlic." *Asia Pacific Journal of Clinical Nutrition* 17 (2008).

Seki, Taiichiro, Takashi Hosono, Tomomi Hosono-Fukao, Kahoru Inada, Rie Tanaka, Jun Ogihara, and Toyohiko Ariga. "Anticancer effects of diallyl trisulfide derived from garlic." *Asia Pacific Journal of Clinical Nutrition* 17 (2008).

Seki, Taiichiro, Takashi Hosono, Tomomi Hosono-Fukao, Kahoru Inada, Rie Tanaka, Jun Ogihara, and Toyohiko Ariga. "Anticancer effects of diallyl trisulfide derived from garlic." *Asia Pacific Journal of Clinical Nutrition* 17 (2008).

Todd, John A., Edward J. Modest, Peter W. Rossow, and Zoltán A. Tökés. "Liposome encapsulation enhancement of methotrexate sensitivity in a transport resistant human leukemic cell line." *Biochemical Pharmacology* 31, no. 4 (1982): 541-546.Vignesh V, Anbarasi K.R, Sathiyanarayanan G, Subramanian P, Khan, Mohammad Naved, Tabrez Alam Khan, Zaheer Khan, and Shaeel Ahmed Al-Thabaiti. "Green synthesis of biogenic silver nanomaterials using Raphanus sativus extract, effects of stabilizers on the morphology, and their antimicrobial activities." *Bioprocess and biosystems engineering* 38 (2015): 2397-2416.

Wettasinghe, Mahinda, and Fereidoon Shahidi. "Scavenging of reactive-oxygen species and DPPH free radicals by extracts of borage and evening primrose meals." *Food chemistry* 70, no. 1 (2000): 17-26.